

Modeling Dielectric Interfaces in the FDTD-Method: A Comparative Study

C. H. Teng, A. Ditkowski, J. S. Hesthaven

Abstract—In this paper, we present special finite difference schemes embedded in the Cartesian Yee cell algorithm for modeling dielectric materials with curved interfaces. The accuracy and efficiency of the new method is demonstrated by numerical computations. We also compare the performance of the new approach and more traditional staircase formulations with and without accuracy improving techniques. These techniques are basically using averaged material properties at staircased interfaces. The numerical results show that the traditional techniques can improve the accuracy of the solution only for electromagnetic fields being continuous at the interface. On the other hand, numerical results obtained by the new methods are more accurate than those obtained by the others. Most importantly, the solutions are second order accurate even for electromagnetic fields being discontinuous at the interface.

Keywords—Finite difference schemes, Maxwells equations, Complex geometries, dielectric interfaces, Staircasing

I. INTRODUCTION

USING the classical finite difference time domain (FDTD) method to simulate the interaction of electromagnetic (EM) waves with geometrically complex objects, one very often encounters that a simple Cartesian grid mesh fails to properly describe the boundaries of the object, e.g., material interfaces and metallic boundaries. A standard approach to overcoming this problem is to use staircase boundaries which roughly approximate actual boundaries. Hence the problem is forced to conform to the simple grid structure. It is well known, however, that this approach has a severe impact on the overall scheme. It reduces the scheme to at best first-order accuracy, and allows the possibility of localized non-convergent behavior.

Several techniques have been proposed in the past to ameliorate this unfortunate situation. For either the whole domain or close to the object, the straightforward approach is to use irregular nonorthogonal grids or curvilinear coordinates; instead of the simple Cartesian Yee cell. Clearly, this is much more complicated as compared to the simple FDTD approach. Emphasizing simplicity, an alternative approach, centered around the idea of defining averaged material properties at the staircase material interfaces, has been used extensively in the past. It yields superior results when compared to utilizing only the staircase formulation.

However, in [6], [7], it has been shown that using the staircase approximation may have a serious consequence:

C. H. Teng is at the Division of Applied Mathematics, Brown University, Providence, RI 02912 E-mail: ct@cfm.brown.edu

A. Ditkowski is at the Division of Applied Mathematics, Brown University, Providence, RI 02912 E-mail: adit@cfm.brown.edu

J. S. Hesthaven is at the Division of Applied Mathematics, Brown University, Providence, RI 02912 E-mail: JAN_HESTHAVEN@BROWN.EDU.

the non-convergence of the scheme has been proven by rigorous mathematical analysis and numerical computations. Moreover, they also developed a general framework for designing new schemes to use at the grid points near the boundaries in the Cartesian Yee cell. These new schemes are constructed by combining both the one-sided difference operator and the boundary conditions. Applying the new method, one does not need to use the staircase approximation and hence overcomes the problems induced by it. Most importantly, the numerical solutions converge at a second-order rate in L_2 .

In this paper, following the same ideas as in [6], [7], we present novel schemes for simulating two dimensional EM wave phenomenon involving dielectric material interfaces, where EM fields can be either continuous or discontinuous. The performance of the new method is demonstrated by numerically solving scattering of EM waves by a dielectric cylinder, for both transverse electric (TE) and transverse magnetic (TM) modes. Our results show that these schemes are capable of handling such tasks and producing solutions with second-order accuracy in L_2 . We also test several traditional approaches, the staircase approximation and the averaging techniques, by the same experiments. From the results, we observe that the traditional methods can improve the accuracy *only* for EM fields being continuous at the dielectric interface.

The paper is organized as follows. In the next section, we start with a general physical problem formulated by Maxwell's equations subjected to the dielectric material interface boundary conditions. We then discuss several traditional approaches, and the formulation of the new schemes in greater detail. The numerical results from all these methods are presented in Section 3. Implementation issues and the efficiency of the new methods are also discussed. In the last section, we address some concluding remarks and ideas for future work.

II. FORMULATION

A. Maxwell's equations and Yee schemes

Consider two media meeting at an interface as shown in Fig.(1). For simplicity, we assume that each medium is characterized by a constant permittivity ϵ and a constant permeability μ . In the media, the EM wave phenomenon is governed by Maxwell's equations and the boundary conditions at the interface.

Without losing generality, let us consider the Maxwell's equations for the TE waves in two dimension of the form,

$$\epsilon_\alpha \partial_t E_{z,\alpha} = \partial_x H_{y,\alpha} \quad , \quad (1)$$

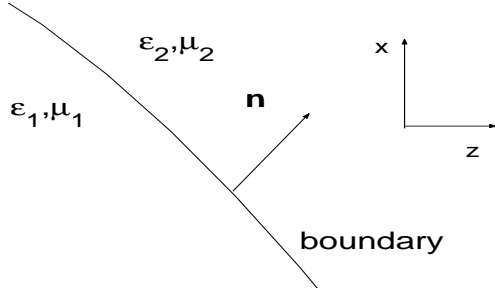


Fig. 1.

$$\epsilon_{\alpha} \partial_t E_{x,\alpha} = -\partial_z H_{y,\alpha} \quad , \quad (2)$$

$$\mu_{\alpha} \partial_t H_{y,\alpha} = \partial_x E_{z,\alpha} - \partial_z E_{x,\alpha} \quad , \quad (3)$$

where $\alpha = 1, 2$ denote different materials. The variables, E_z, E_x and H_y , are the electric and magnetic field components. The boundary conditions at the interface are

$$n_z E_{x,1} - n_x E_{z,1} = n_z E_{x,2} - n_x E_{z,2} \quad , \quad (4)$$

$$\epsilon_1 (n_z E_{z,1} + n_x E_{x,1}) = \epsilon_2 (n_z E_{z,2} + n_x E_{x,2}) \quad , \quad (5)$$

$$H_{y,1} = H_{y,2} \quad , \quad (6)$$

where n_z and n_x are the z and x components of a unit normal vector \mathbf{n} , pointing outward from material 1 to 2.

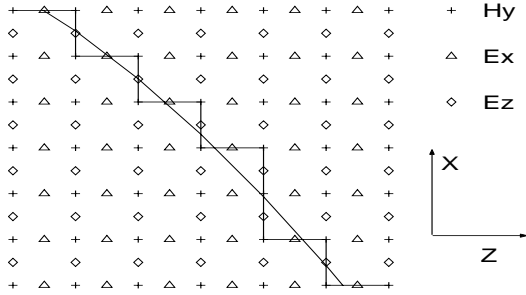


Fig. 2.

To solve the set of equations by the FDTD method, a two dimensional staggered grid mesh is constructed by the tensor product of the grid points defined as

$$z_i = \Delta z(i), \quad z_{i+\frac{1}{2}} = \Delta z(i + \frac{1}{2}),$$

$$x_j = \Delta x(j), \quad x_{j+\frac{1}{2}} = \Delta x(j + \frac{1}{2}),$$

where Δz and Δx denote the grid sizes in z and x directions. An illustration of the mesh is given in Fig.(2). Let $E_{z_{i+\frac{1}{2},j}}$, $E_{x_{i,j+\frac{1}{2}}}$ and $H_{y_{i+\frac{1}{2},j+\frac{1}{2}}}$ be the values of the EM field components evaluated at the grid points:

$$E_{z_{i+\frac{1}{2},j}} = E_z(z_{i+\frac{1}{2}}, x_j)$$

$$E_{x_{i,j+\frac{1}{2}}} = E_x(z_i, x_{j+\frac{1}{2}})$$

$$H_{y_{i+\frac{1}{2},j+\frac{1}{2}}} = H_y(z_{i+\frac{1}{2}}, x_{j+\frac{1}{2}}).$$

Replacing the spatial derivatives in Maxwell's equation by the central difference approximations yields

$$\epsilon_{i+\frac{1}{2},j} \frac{d}{dt} E_{z_{i+\frac{1}{2},j}} = \frac{H_{y_{i+\frac{1}{2},j+\frac{1}{2}}} - H_{y_{i+\frac{1}{2},j-\frac{1}{2}}}}{\Delta x} \quad , \quad (7)$$

$$\epsilon_{i,j+\frac{1}{2}} \frac{d}{dt} E_{x_{i,j+\frac{1}{2}}} = -\frac{H_{y_{i+\frac{1}{2},j+\frac{1}{2}}} - H_{y_{i-\frac{1}{2},j+\frac{1}{2}}}}{\Delta z} \quad (8)$$

$$\mu_{i+\frac{1}{2},j+\frac{1}{2}} \frac{d}{dt} H_{y_{i+\frac{1}{2},j+\frac{1}{2}}} = \frac{E_{z_{i+\frac{1}{2},j+1}} - E_{z_{i+\frac{1}{2},j}}}{\Delta x} - \frac{E_{x_{i+1,j+\frac{1}{2}}} - E_{x_{i,j+\frac{1}{2}}}}{\Delta z}. \quad (9)$$

In the Eq.(7), (8) and (9), $\epsilon_{i+\frac{1}{2},j}$, $\epsilon_{i,j+\frac{1}{2}}$ and $\mu_{i+\frac{1}{2},j+\frac{1}{2}}$ are the values of the material properties of the medium in each region. It is well known that solving the system numerically does not give promising results due to the staircase formulation. We would like to discuss some techniques, using the averaged constitution parameters at the staircase interface, to improve the accuracy. To distinguish with the other approaches given later, the staircase approximation without using modified material properties will be referred as method one.

B. Classical techniques: averaging methods

The averaging method is very simple to apply. For grid points at the staircase interface, it basically reassigns the values of $\epsilon_{i+\frac{1}{2},j}$, $\epsilon_{i,j+\frac{1}{2}}$ and $\mu_{i+\frac{1}{2},j+\frac{1}{2}}$ by some formulas. The formulas are taking mean values of the material properties under some specific considerations. Hence, applying the methods in a pre-stage, one can use the same Yee algorithm as usual. We would like to discuss three commonly used averaging techniques. The three formulas referred as method 2,3 and 4 are:

Method 2

$$\epsilon_{eff} = \frac{\epsilon_1 + \epsilon_2}{2}, \quad \mu_{eff} = \frac{\mu_1 + \mu_2}{2}. \quad (10)$$

Method 3

$$\epsilon_{eff} = \left(\frac{\sqrt{\epsilon_1} + \sqrt{\epsilon_2}}{2}\right)^2, \quad \mu_{eff} = \left(\frac{\sqrt{\mu_1} + \sqrt{\mu_2}}{2}\right)^2. \quad (11)$$

Method 4 (harmonic mean)

$$\epsilon_{eff} = \frac{2\epsilon_1\epsilon_2}{\epsilon_1 + \epsilon_2}, \quad \mu_{eff} = \frac{2\mu_1\mu_2}{\mu_1 + \mu_2} \quad (12)$$

In method 2, the arithmetic mean of the material parameters is used, which results in a smooth change of the parameters at the interface instead of a step jump. One can also use the mean of the phase speeds of the electromagnetic waves traveling in different media. In method 3, we use the formulas for either ϵ or μ being the same in different media, e.g., a non-magnetic medium placed in free space.

All these techniques share the advantage of the simplicity of the Yee scheme. However, they all suffer some drawbacks due to the staircasing approximation from the following points of view. Because of the failure of describing

the curved interface, the information such as the location of the curved interface in the mesh is changed. Consequently, the normal vector at the interface, which is needed in the boundary conditions, are incorrectly set to directions parallel to grid axes. Furthermore, the flux at each interface grid point, where the derivatives of the fields may not be continuous in general, are evaluated by using values from each region. As a result, one should not expect that such an approach will always give accurate solutions.

C. Special schemes at grid points near the interface

After introducing the classical approaches for improving the computations, we would like to apply the ideas proposed in [6] to overcoming the improper situations. Our purpose is to design new schemes for grids near the interface. To complete this task, it is necessary to classify different configurations of how the boundary intersects the staggered grid mesh.

Consider a magnetic field point and the nearest four electric field points as a group. When an interface passes through the group of points, it separates some electric field points and the magnetic field point into different media. We may use this character, the number of electric field points separated from the group, to classify the configurations into two different classes. Two examples from each class are presented in Fig.(3), (4). We will use these configurations as examples to demonstrate the ideas for constructing the new schemes.

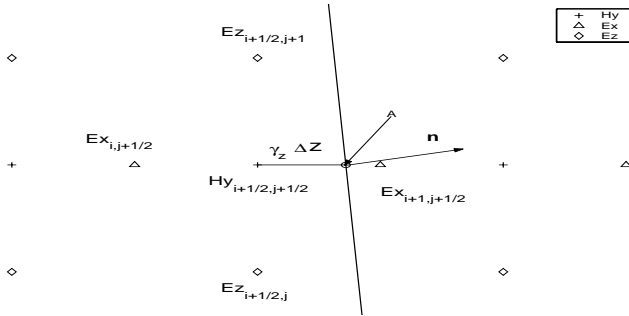


Fig. 3. Type 1 configuration

The character of the first class is that the boundary separates one electric field point to the rest of the four. As shown in Fig.(3), the interface intersects the line connecting $H_{y_{i+\frac{1}{2}, j+\frac{1}{2}}}$ and $E_{x_{i+1, j+\frac{1}{2}}}$ at point A and thus $E_{x_{i+1, j+\frac{1}{2}}}$ is separate from the group. Note that $\gamma_z \Delta z$ denotes the distance from $H_{y_{i+\frac{1}{2}, j+\frac{1}{2}}}$ to point A. In another word, γ_z is the ratio of the distance to the grid size in z direction. Due to the separation, we need to construct schemes for updating the values at $H_{y_{i+\frac{1}{2}, j+\frac{1}{2}}}$ and $E_{x_{i+1, j+\frac{1}{2}}}$. The algorithms for updating $H_{y_{i+\frac{1}{2}, j+\frac{1}{2}}}$ and $E_{x_{i+1, j+\frac{1}{2}}}$ in this kind of configuration have been introduced in [6]. In here, we would like to show a simplified version.

The scheme for updating $H_{y_{i+\frac{1}{2}, j+\frac{1}{2}}}$ is

$$\mu_{i+\frac{1}{2}, j+\frac{1}{2}} \frac{d}{dt} H_{y_{i+\frac{1}{2}, j+\frac{1}{2}}} = \frac{E_{z_{i+\frac{1}{2}, j+1}} - E_{z_{i+\frac{1}{2}, j}}}{\Delta x} - \frac{2}{2\gamma_z + 1} \frac{E_{x,1} - E_{x_{i, j+\frac{1}{2}}}}{\Delta z}. \quad (13)$$

where $E_{x,1}$ is the field value at the boundary point A in medium one. Comparing the two schemes, (9)(13), one see that a one-sided difference operator is used in (13), instead of a central difference operator as in (9). As a consequence, Eq.(13) contains additional information, the distance of the interface to the $H_{y_{i+\frac{1}{2}, j+\frac{1}{2}}}$ in z direction characterized by γ_z . To use Eq.(13), one needs to provide the value of $E_{x,1}$ which is, unfortunately, not given from the physical problem. However, we can utilize the boundary conditions and the nearby field values to estimate the value of $E_{x,1}$. From the boundary conditions Eq.(4) and (5) at point A, we can write $E_{x,1}$ as

$$E_{x,1} = \frac{\epsilon_2}{\epsilon_1 n_x^2 + \epsilon_2 n_z^2} E_{x,2} + \frac{(\epsilon_2 - \epsilon_1) n_z n_x}{\epsilon_1 n_x^2 + \epsilon_2 n_z^2} E_{z,1}. \quad (14)$$

In Eq.(14), it implies that one can approximate the values of $E_{x,2}$ and $E_{z,1}$ first, and then substitute the two values into Eq.(14) to estimate the value of $E_{x,1}$. To approximate the values of $E_{x,2}$ and $E_{z,1}$, we can use extrapolation and interpolation of the nearby field values. The formulas are:

$$E_{x,2} = \left(\frac{3}{2} - \gamma_z\right) E_{x_{i+1, j+\frac{1}{2}}} - \left(\frac{1}{2} - \gamma_z\right) E_{x_{i+2, j+\frac{1}{2}}}, \quad (15)$$

$$E_{z,1} = (1 + \gamma_z) \left(\frac{E_{z_{i+\frac{1}{2}, j+1}} + E_{z_{i+\frac{1}{2}, j-1}}}{2} \right) - \gamma_z \left(\frac{E_{z_{i-\frac{1}{2}, j+1}} + E_{z_{i-\frac{1}{2}, j-1}}}{2} \right). \quad (16)$$

Therefore, the value of $E_{x,1}$ at point A is obtained by using Eq. (14), (15) and (16), and one can use Eq.(13) to update $H_{y_{i+\frac{1}{2}, j+\frac{1}{2}}}$.

To update $E_{x_{i+1, j+\frac{1}{2}}}$, one simply use the following scheme,

$$\epsilon_{i+1, j+\frac{1}{2}} \frac{d}{dt} E_{x_{i+1, j+\frac{1}{2}}} = \frac{-2}{(2\tilde{\gamma}_z + 1)} \frac{H_{y_{i+\frac{3}{2}, j+\frac{1}{2}}} - H_{y,2}}{\Delta z}, \quad (17)$$

where $\tilde{\gamma}_z = \frac{1}{2} - \gamma_z$. The variable $H_{y,2}$ is the magnetic field value at point A in medium two. Here, we encounter a similar problem, not knowing the value of $H_{y,2}$. However, we can follow the same procedure to estimate the value of $E_{x,1}$. The resulting formula is given as

$$H_{y,2} = H_{y,1} = (1 + \tilde{\gamma}_z) H_{y_{i+\frac{1}{2}, j+\frac{1}{2}}} - \tilde{\gamma}_z H_{y_{i-\frac{1}{2}, j+\frac{1}{2}}}. \quad (18)$$

Finally, we have presented the schemes for updating $H_{y_{i+\frac{1}{2}, j+\frac{1}{2}}}$ and $E_{x_{i+1, j+\frac{1}{2}}}$ and the auxiliary schemes to use them. To handle all the configurations in the first class,

three other sets of algorithms are needed. Each one is used in the configuration when $E_{z_{i+\frac{1}{2},j+1}}$, $E_{x_{i,j+\frac{1}{2}}}$ or $E_{z_{i+\frac{1}{2},j}}$ is separated from $H_{y_{i+\frac{1}{2},j+\frac{1}{2}}}$ by the interface, and all the schemes can be constructed by the same procedure presented here.

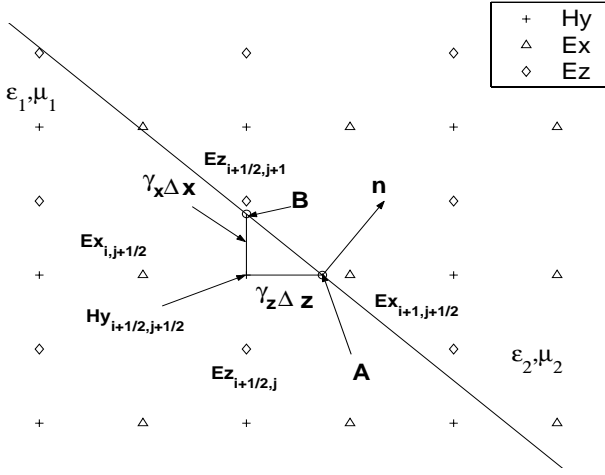


Fig. 4. Type 2 configuration

The character of the second class is that two electric field points are separated from the group of points. A typical configuration in the second class is shown in Fig.(4). In Fig.(4), the interface intersects one line, connecting $H_{y_{i+\frac{1}{2},j+\frac{1}{2}}}$ and $E_{x_{i+1,j+\frac{1}{2}}}$, at point A, and another line, connecting $H_{y_{i+\frac{1}{2},j+\frac{1}{2}}}$ and $E_{z_{i+\frac{1}{2},j+1}}$, at point B. We can now characterize this configuration by γ_z and γ_x , where $\gamma_z\Delta z$ and $\gamma_x\Delta x$ are the distances from $H_{y_{i+\frac{1}{2},j+\frac{1}{2}}}$ to point A and B. In this configuration, we need to design schemes for updating the field values, $H_{y_{i+\frac{1}{2},j+\frac{1}{2}}}$, $E_{x_{i+1,j+\frac{1}{2}}}$ and $E_{z_{i+\frac{1}{2},j+1}}$.

Comparing the two configurations, one observes that the situations of $E_{x_{i+1,j+\frac{1}{2}}}$ and $E_{z_{i+\frac{1}{2},j+1}}$ in Fig.(4) are similar to the situation of $E_{x_{i+1,j+\frac{1}{2}}}$ in Fig.(3). Hence, we can use Eq.(17) and (18) to update $E_{x_{i+1,j+\frac{1}{2}}}$ directly, and $E_{z_{i+\frac{1}{2},j+1}}$ after changing the variables and the corresponding grid indices. Therefore, we only have to consider how to construct the set of schemes for updating $H_{y_{i+\frac{1}{2},j+\frac{1}{2}}}$.

Following the same procedure developed previously, we have a scheme for updating $H_{y_{i+\frac{1}{2},j+\frac{1}{2}}}$ as

$$\mu_{i+\frac{1}{2},j+\frac{1}{2}} \frac{d}{dt} H_{y_{i+\frac{1}{2},j+\frac{1}{2}}} = \frac{2}{2\gamma_x + 1} \frac{E_{z,1} - E_{z_{i+\frac{1}{2},j}}}{\Delta x} - \frac{2}{2\gamma_z + 1} \frac{E_{x,1} - E_{x_{i,j+\frac{1}{2}}}}{\Delta z}, \quad (19)$$

where the $E_{x,1}$ and $E_{z,1}$ are field values at point A and B in medium one. As before, since the values of $E_{x,1}$ and $E_{z,1}$ are not known, we need to find a way to approximate them.

Let us first consider how to find $E_{x,1}$. If we try to estimate $E_{x,1}$ using Eq.(14),(16) and (15) developed in the previous case, we immediately know that Eq.(16) is no longer

valid. The reason is that the average of E_z can not be used due to different media. However, one may try another approach to approximate $E_{x,1}$. From the boundary conditions (4),(5), $E_{x,1}$ can be written as

$$E_{x,1} = \frac{\epsilon_1 n_z^2 + \epsilon_2 n_x^2}{\epsilon_1} E_{x,2} + \frac{\epsilon_2 - \epsilon_1}{\epsilon_1} n_z n_x E_{z,2}. \quad (20)$$

To estimate the value of $E_{x,1}$, we can substitute two approximated values of $E_{x,2}$ and $E_{z,2}$ into Eq.(20), and thus two auxiliary equations are needed. Fortunately, since we can approximate $E_{x,2}$ by Eq.(15), we only need to derive an auxiliary equation for $E_{z,2}$, and the procedure is the following. We evaluate one interpolated value of E_z field at the coordinate $(z_{i+1/2} + \gamma_z\Delta z, x_{j+1})$ using $E_{z_{i+\frac{1}{2},j+1}}$ and $E_{z_{i+\frac{3}{2},j+1}}$, and another one at the coordinate $(z_{i+1/2} + \gamma_z\Delta z, x_{j+2})$ using $E_{z_{i+\frac{1}{2},j+2}}$ and $E_{z_{i+\frac{3}{2},j+2}}$. We then use the interpolated values to computed a extrapolated value, $E_{z,2}$ at point A. Hence, the expression of the auxiliary equation for $E_{z,2}$ is

$$E_{z,2} = \frac{3}{2} (E_{z_{i+\frac{1}{2},j+1}} + \gamma_z (E_{z_{i+\frac{3}{2},j+1}} - E_{z_{i+\frac{1}{2},j+1}})) - \frac{1}{2} (E_{z_{i+\frac{1}{2},j+2}} + \gamma_z (E_{z_{i+\frac{3}{2},j+2}} - E_{z_{i+\frac{1}{2},j+2}})). \quad (21)$$

Therefore, using Eq.(20), (15) and (21), we have $E_{x,1}$ for Eq.(19).

To estimate the value of $E_{z,1}$ at point B, we can perform a similar procedure as for the value of $E_{z,1}$. Hence, we directly present the auxiliary equations:

$$E_{z,1} = \frac{\epsilon_1 n_z^2 + \epsilon_2 n_x^2}{\epsilon_1} E_{z,2} + \frac{\epsilon_2 - \epsilon_1}{\epsilon_1} n_z n_x E_{x,2}. \quad (22)$$

$$E_{z,2} = \left(\frac{3}{2} - \gamma_x\right) E_{z_{i+\frac{1}{2},j+1}} - \left(\frac{1}{2} - \gamma_x\right) E_{z_{i+\frac{1}{2},j+2}}, \quad (23)$$

$$E_{x,2} = \frac{3}{2} (E_{x_{i+1,j+\frac{1}{2}}} + \gamma_x (E_{x_{i+1,j+\frac{3}{2}}} - E_{x_{i+1,j+\frac{1}{2}}})) - \frac{1}{2} (E_{x_{i+2,j+\frac{1}{2}}} + \gamma_x (E_{x_{i+2,j+\frac{3}{2}}} - E_{x_{i+2,j+\frac{1}{2}}}). \quad (24)$$

After giving the equations for estimating $E_{x,1}$ and $E_{z,1}$, we can use them with Eq.(19) to update $H_{y_{i+\frac{1}{2},j+\frac{1}{2}}}$.

We have discussed the schemes for updating the three field values. As in the first case, we also need three other sets of algorithms to handle all the configurations in the second class. The schemes are constructed in a similar fashion for computing field values, when $E_{z_{i+\frac{1}{2},j+2}}$ and $E_{z_{i+\frac{1}{2},j+2}}$, $E_{z_{i+\frac{1}{2},j+2}}$ and $E_{z_{i+\frac{1}{2},j+2}}$, or $E_{z_{i+\frac{1}{2},j+2}}$ and $E_{z_{i+\frac{1}{2},j+2}}$ are not placed in the same medium with $H_{y_{i+\frac{1}{2},j+\frac{1}{2}}}$.

III. NUMERICAL COMPUTATION AND DISCUSSION

To compare the performance of all the methods mentioned in the previous section, we use them to solve a fundamental physical problem, scattering by a dielectric cylinder in free space with TE and TM wave excitations. The reasons of choosing this simple problem are the following. First, the problem has an exact solution. Hence, we can

measure the errors in the numerical solutions computed by all the methods. The second reason is that the scatterer has a curved boundary. Hence, we will know if the new schemes have the capability of handling complex geometries. The last one is to demonstrate how well the methods perform when EM waves are either continuous or discontinuous at the interface.

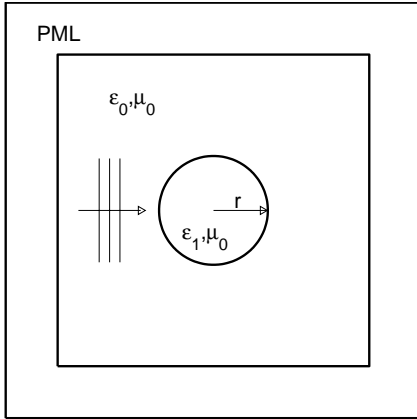


Fig. 5.

The computation is setup by using total/scattering field formulation where the range of the total field is $[-1, 1] \times [-1, 1]$. Inside the total field region, a dielectric cylinder is placed at the center. To simulate the outgoing waves in the finite computational domain, a perfect matched layer (PML) type absorbing boundary condition [5] is used. An illustration is shown in Fig.(5). In the numerical test, we use the following parameters. The permittivity and permeability in free space are given as $\epsilon_0 = 1$ and $\mu_0 = 1$. The material properties and the radius of the cylinder are $\epsilon_d = 2\epsilon_0$, $\mu_d = \mu_0$, and $r = (\pi/6)$. The incident waves are time-harmonic fields. The angular frequency is equal to 2π and the amplitude as well as the wavelength λ_0 measured in free space are set to unity.

All the schemes presented in Section 2 are in semi-discrete form. To update the field values in time, we use the fourth-order Runge-Kutta algorithm in all five methods. The time step used in the computations is

$$\Delta t = \frac{\min(\Delta z, \Delta x)}{\sqrt{2}c} \quad (25)$$

where c is the speed of light after normalization. Therefore, c is equal to one in this particular case. In all the computations, we let $\Delta z = \Delta x = h$ during mesh refinement and compute the time step adaptively by Eq.(25).

To compare the performances of different methods, we measure the discrete L_2 error, $\|\delta U\|_h$, defined as

$$\|\delta U\|_h = \sqrt{\Delta z \Delta x \sum_{i,j} (U_{i,j} - U_{exact})^2}. \quad (26)$$

The variable $U_{i,j}$ is the field value computed at the grid point, and U_{exact} refers to exact one. The analytic solutions to this particular problem can be found in [1].

All the computations are marched to $t=20$ where the numerical solutions have reach a periodic pattern. We then measure the discrete L_2 errors at that time. The resolution of the numerical solution is characterized by N , the number of points per wavelength (ppw) measured from the incident wave. The error versus N ppw of the EM fields are shown in Fig.(6),(7) and (8) for the TE mode, and Fig.(9),(10) and (11) for the TM mode.

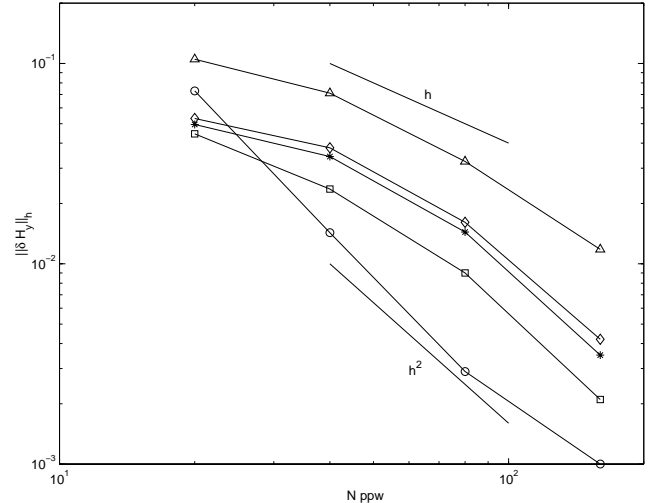


Fig. 6. The discrete L_2 errors of H_y by the different methods: \triangle : staircase, \diamond : $(\epsilon_1 + \epsilon_2)/2$, $*$: $((\sqrt{\epsilon_1} + \sqrt{\epsilon_2})/2)^2$, \square : $2\epsilon_1\epsilon_2/(\epsilon_1 + \epsilon_2)$, \circ : new method.

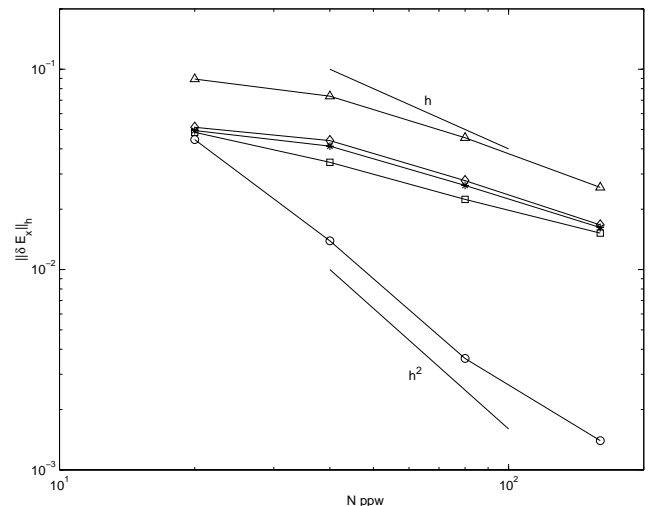


Fig. 7. The discrete L_2 errors of E_x by the different methods: \triangle : staircase, \diamond : $(\epsilon_1 + \epsilon_2)/2$, $*$: $((\sqrt{\epsilon_1} + \sqrt{\epsilon_2})/2)^2$, \square : $2\epsilon_1\epsilon_2/(\epsilon_1 + \epsilon_2)$, \circ : new method.

Let us examine the errors of the H_y field from the TE waves in Fig.(6). It shows that the staircase approximation has the largest error among all the methods for the same N . Moreover, the numerical solutions computed by the method converge slowly, from $O(h)$ to $O(h\sqrt{h})$ as N increases. The results obtained by the averaging methods show that the techniques do improve the accuracy of the

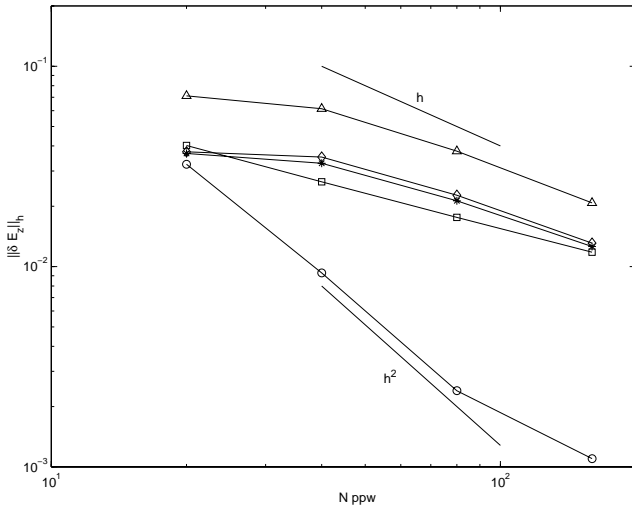


Fig. 8. The discrete L_2 errors of E_z by the different methods:
 Δ : staircase, \diamond : $(\epsilon_1 + \epsilon_2)/2$, $*$: $((\sqrt{\epsilon_1} + \sqrt{\epsilon_2})/2)^2$
 \square : $2\epsilon_1\epsilon_2/(\epsilon_1 + \epsilon_2)$, \circ : new method.

numerical solutions. We also observe that the errors decay to second order for N being large. The numerical solutions obtained by the new method are the most accurate when EM waves are well resolved. Moreover, the errors decay by a factor of four as N increases twice. This indicates that the new methods are second order accurate except for $N = 160$ ppw, and the exception is due to the reflection from the PML.

In Fig.(7) and (8), we present the results from the E_x and E_z field computation. As shown in both figures, the performance of the staircase formulation is very poor and the numerical solutions are less than first order accurate. Unfortunately, the averaging methods can only reduce the errors approximately by half but fail to improve the order of accuracy of the methods as in the H_y field computations. The reason for the convergence rates being so slow is that the staircase formulation fails to correctly model the discontinuities of E_x and E_z fields at the interface. On the other hand, the new method does not have such problems and the results obtained by that are second order accurate. Due to different convergence rates, for both E_z and E_x fields, the new method has the L_2 errors approximately one order of magnitude lower than the others for $N = 80$ ppw.

Let us turn our attention to the TM mode, a case where all the EM fields are continuous at the boundary. In Fig.(9),(10) and (11), the results show that the solutions are only first order accurate for staircase approximation. Using the harmonic mean of the material parameters gives less error and the order of accuracy is recover for large N ppw. When using the new method, one observes that the errors are of second order and the smallest among all other methods.

The new method is also more efficient than the others, when one demands the error in the numerical solution to be lower than a certain level. For instance, let us consider

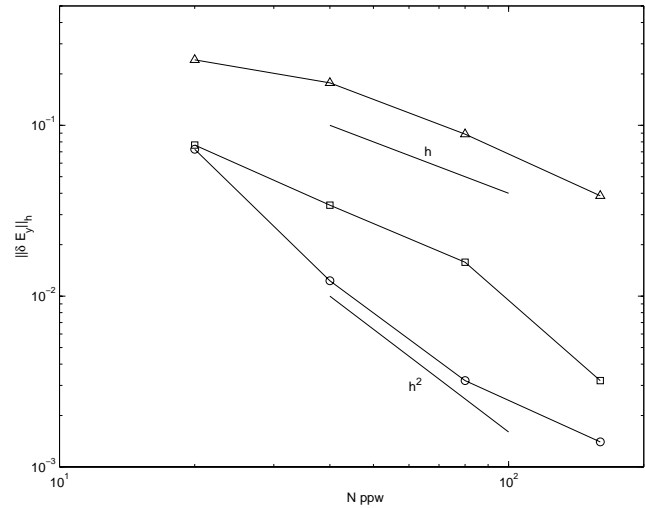


Fig. 9. The discrete L_2 errors of E_y by different methods:
 Δ : staircase, \square : $2\epsilon_1\epsilon_2/(\epsilon_1 + \epsilon_2)$, \circ : new method.

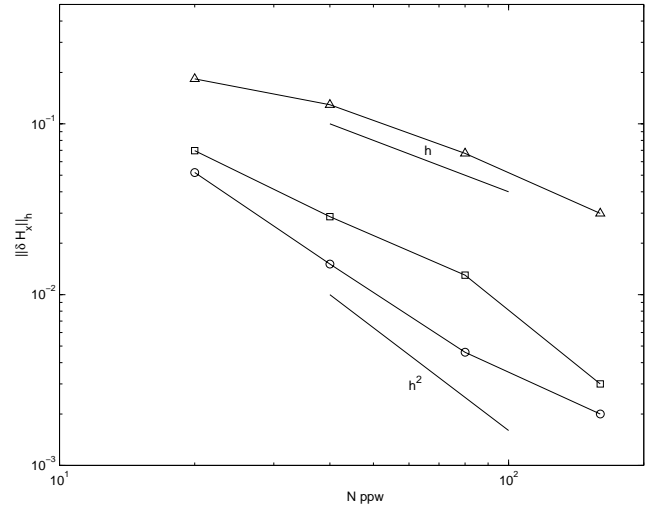


Fig. 10. The discrete L_2 errors of H_x by different methods:
 Δ : staircase, \square : $2\epsilon_1\epsilon_2/(\epsilon_1 + \epsilon_2)$, \circ : new method.

the global L_2 error to be around 0.01, which can be viewed as 1% relative error defined as the ratio of the L_2 error to the amplitude of the incident wave. Under such request for the TE mode, one sees that 40 ppw will be enough for the new method but 160 ppw for the others due to the discontinuous fields. Hence, the computation memory and the total time for computing derivatives are reduced by 16 times when the new method is used. Moreover, since the grid sizes in the new method are 4 times larger than those in the other methods, the time step is also 4 times larger. Therefore, the new method gives results 64 time faster than the others, due to the saving combined from the temporal and spatial part theoretically. Similarly, for TM mode, we need to use 40 ppw for the new method but 80 ppw for the traditional ones to satisfy the same accuracy request. Hence, the new method is still 8 times faster than the traditional methods. However, to gain all these advantages,

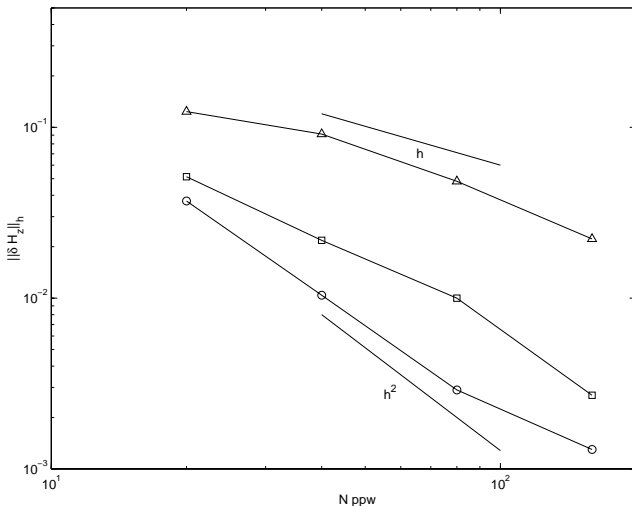


Fig. 11. The discrete L_2 errors of H_z by different methods: Δ : staircase, \square : $2\epsilon_1\epsilon_2/(\epsilon_1 + \epsilon_2)$, \circ : new method.

an additional workload, flux correction for the grids near the boundary, is required. Hence, it is necessary to know how this additional part affect the computations. To explain the effect of the additional workload, implementation issues are discussed in the next.

To update field values by special schemes, one needs the corresponding values of γ_z , γ_x and the normal vectors. Fortunately, all these values only need to be computed once and stored in a pre-stage. With all the values in hand, one first computes the derivatives at all the grid points as in the traditional methods, and then add an additional stage to recompute the derivatives at the grid points using special schemes. The procedure given here is suitable when the Runge-Kutta method in time is used. If the Leap Frog scheme staggered in time is used, then one may use the following procedure. The first step is to update the field values at the special grid points using the new method, and store them in an additional array. Then we update the field values at every grid point as usual. The last step is to replace new field values at the special grid points by the values obtained in the first one. Although the derivatives are computed twice at the grid points near the boundary, the additional work is much less than the work for computing derivatives for all the grid points. This is due to the fact that the total number of the special grid points and all the grid points being $O(N)$ and $O(N^2)$ respectively.

In table (I), a direct measurement of the total CPU time of three computations terminated at time $t = 20$ is provided. Surprisingly, as shown in the table, the total CPU time by the new method and the traditional method are only one second in difference for computation using $N = 40$ ppw. In another word, adding an additional 0.1% workload relative to the traditional method gives all the advantages mentioned above. In the table, it is shown that using new methods with 40 ppw is 68 times faster than using traditional method with 160 ppw.

Method	N ppw	CPU time (sec)	$\ \delta E_x\ _h$	$\ \delta E_z\ _h$
New	40	878	0.0139	0.0093
Method 4	40	877	0.0343	0.0265
Method 4	160	59871	0.0152	0.0118

TABLE I

A MEASUREMENT OF THE TOTAL CPU TIME BY DIFFERENT METHODS FOR TE MODE WITH L_2 ERROR AROUND 0.01

IV. CONCLUSIONS

In this paper, we present a new approach to model the dielectric interface in the FDTD method. We compare the new method to the classical staircase formulation with and without averaging techniques. The results show that the averaging techniques can only improve the accuracy of numerical solutions when the EM fields at the interface are continuous. On the other hand, the results obtained by the new methods are of second order accurate, and thus much more accurate than those computed by the other methods. The numerical evidences indicate that the new method is indeed capable of simulating the EM waves being continuous and discontinuous at the curved interface.

Applying the same idea presented here, one can construct special schemes to improve the existing algorithms. Currently, special schemes for higher dimension and high order algorithms are under investigation. We hope to report such applications in the future.

ACKNOWLEDGMENTS

This work was partially supported by AFOSR grant F49620-96-1-0426, NSF grant DMS-0074257, and DOE grant 98-ER-25346. JSH acknowledges partial support as a Sloan Research Fellow from the Sloan Foundation.

REFERENCES

- [1] R. F. Harrington, *Time-Harmonic Electromagnetic Fields*, McGraw-Hill Book Company, Inc. 1961.
- [2] K. S. Yee, *Numerical Solution of Initial Boundary Value Problems Involving Maxwell's Equations in Isotropic Media*, IEEE Trans. Antennas Propag. 14, 1966.
- [3] K. S. Kunz and R.J. Luebbers, *The Finite Difference Time Domain Method for Electromagnetics*, CRC Press, Inc., 1993.
- [4] A. Taflov, *Computational Electrodynamics, The Finite Difference Time Domain Method*, Artech House, Norwood, MA, 1995.
- [5] J. S. Hesthaven, P.G. Dinesen, and J.P. Lynov, *Spectral Collocation Time-Domain Modeling of Diffractive Optical Elements*, J. Comput. Phys. 1999 - to appear
- [6] A. Ditkowski, K. Dridi and J.S. Hesthaven *Convergent Cartesian Grid Methods for Maxwell's Equations in Complex Geometries*, Journal of Computational Physics, 2000 - to appear.
- [7] K. H. Dridi, J.S. Hesthaven and A. Ditkowski, *Staircase Free Finite-Difference Time-Domain Formulation for General Materials in Complex Geometries*, IEEE Trans. Antennas Propagat. 1999 - submitted.